

Nuclear quantum effects in *ab initio* dynamics: Theory and experiments for lithium imideMichele Ceriotti,^{1,*} Giacomo Miceli,^{2,1} Antonino Pietropaolo,³ Daniele Colognesi,⁴ Angeloclaudio Nale,² Michele Catti,² Marco Bernasconi,² and Michele Parrinello¹¹Computational Science, DCHAB, ETH Zurich, USI Campus, via G. Buffi 13, CH-6900 Lugano, Switzerland²Department of Materials Science, Università di Milano-Bicocca, via R. Cozzi 53, I-20125 Milano, Italy³CNISM UdR Roma Tor Vergata and Centro NAST, Università degli Studi di Roma Tor Vergata, via della Ricerca Scientifica 1, I-0133 Roma, Italy⁴Istituto dei Sistemi Complessi, CNR, via Madonna del Piano 10, 50019 Firenze, Italy

(Received 13 September 2010; revised manuscript received 28 October 2010; published 23 November 2010)

Owing to their small mass, hydrogen atoms exhibit strong quantum behavior even at room temperature. Including these effects in first-principles calculations is challenging because of the huge computational effort required by conventional techniques. Here we present the first *ab initio* application of a recently developed stochastic scheme, which allows to approximate nuclear quantum effects inexpensively. The proton momentum distribution of lithium imide, a material of interest for hydrogen storage, was experimentally measured by inelastic neutron-scattering experiments and compared with the outcome of quantum thermostatted *ab initio* dynamics. We obtain favorable agreement between theory and experiments for this purely quantum-mechanical property, thereby demonstrating that it is possible to improve the modeling of complex hydrogen-containing materials without additional computational effort.

DOI: [10.1103/PhysRevB.82.174306](https://doi.org/10.1103/PhysRevB.82.174306)

PACS number(s): 88.30.R-, 71.15.Pd, 78.70.Nx

I. INTRODUCTION

Nuclear quantum effects play an important role in determining the properties of compounds containing light elements, hydrogen in particular. In order to assist the interpretation of experiments, accurate theoretical modeling is highly desirable. Unfortunately, conventional techniques^{1,2} can be orders of magnitude more expensive than methods which treat the nuclei as classical particles. As a consequence, in *ab initio* simulations nuclear quantum effects have seldom been included.^{3,4}

A stochastic molecular-dynamics framework based on generalized Langevin equations has been recently devised. Among the many possible applications,⁵⁻⁷ it allows one to model to a good approximation nuclear quantum effects at negligible additional effort with respect to purely classical dynamics. Preliminary tests based on empirical force fields demonstrated satisfactory agreement with path integral and experimental results.^{6,7}

An additional advantage of this approach is that not only atomic configurations but also the momentum reproduces the quantum distribution. On the contrary, computing the momentum distribution within a path-integral formalism^{2,8} requires special techniques and, despite recent developments,⁹ further increases the computational effort. In the classical limit, the distribution of the momentum \mathbf{p} of a particle is Gaussian, $n(\mathbf{p}) \propto \exp(-\mathbf{p}^2/2mk_B T)$, and depends only on the temperature T and the particle's mass m . Conversely, in a quantum mechanical description $n(\mathbf{p})$ reflects the local potential experienced by the particle. Deviation of the proton momentum distribution (PMD) from the classical one is a very sensitive probe of the quantum-mechanical behavior of hydrogen atoms. Experimental measurements of the PMD have been made feasible since the advent of spallation neutron sources. Indeed, the intense fluxes of neutrons in the 1–100 eV energy range provided by these facilities allows one to study the short time (10^{-16} s) dynamical properties of the proton in different hydrogen containing systems, as well as quantum fluids and solids.¹⁰

In this paper we apply the “quantum thermostat” together with *ab initio* molecular dynamics, in order to model lithium imide. Besides its technological significance as a material for hydrogen storage,^{11,12} Li_2NH is well suited as a benchmark. In fact, the presence of libration modes of the NH bonds is likely to introduce significant anharmonicities, which rule out the possibility of an accurate treatment by harmonic lattice dynamics. Theoretical results are compared with the experimentally determined PMD in lithium imide, which was obtained by means of deep inelastic neutron scattering (DINS) measurements.

II. EXPERIMENTAL DETAILS

DINS measurements were performed on the VESUVIO spectrometer at the ISIS spallation neutron source (Rutherford Appleton Laboratory, United Kingdom),¹³ in the resonance detector configuration and using the foil cycling technique^{14,15} that provides a narrow resolution suitable for line-shape analysis on PMD. The high-energy and wave-vector transfers achievable with DINS allow one to describe the scattering event within the framework of the impulse approximation (IA) with a very high degree of accuracy,^{10,16} so as to extract the proton momentum distribution directly from the experimental data. Actually the value of the wave-vector transfer at the maximum of the proton recoil peak ranges from 35 to 150 \AA^{-1} for the complete set of detectors used in the present experiment. Following Refs. 17 and 18, one can easily evaluate the coefficient which multiplies the first term beyond the impulse approximation, namely, the third derivative of the IA response function itself. Using appropriate physical quantities for lithium imide, one finds (in the low-temperature limit and for the aforementioned values of the wave-vector transfer) that this “final-state effect” coefficient lies in between 3.67 and 0.856 \AA^{-3} . This ensures that the impulse approximation is already reached during the reported neutron-scattering measurement to any practical purpose.

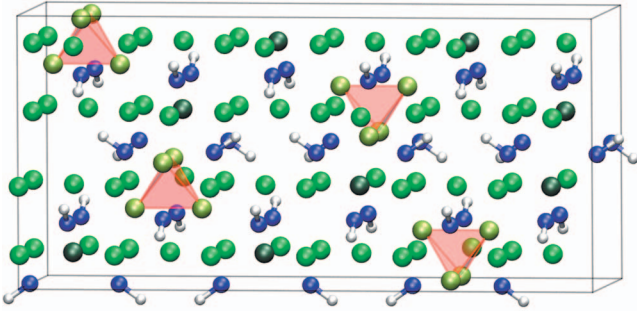


FIG. 1. (Color) A representation of the initial configuration of the atoms in the supercell used for our simulations (Ref. 25). The stable, tetrahedral clusters of interstitial Li atoms are highlighted. Different shades of green correspond to different Wyckoff positions occupied by Li atoms (Ref. 25).

The polycrystalline sample of Li_2NH was synthesized by thermal decomposition of commercial lithium amide (Sigma-Aldrich Inc., reagent grade) at $T=623$ K and $p=10^{-3}$ Pa for 4 h, according to the reaction $\text{LiNH}_2 \rightarrow \frac{1}{2}\text{Li}_2\text{NH} + \frac{1}{2}\text{NH}_3$,^{19,20} in a furnace equipped with turbomolecular vacuum pump. X-ray powder-diffraction measurements (Cu $K\alpha$ radiation) showed the sample to be well crystallized and to contain a small quantity of Li_2O , which was already present in the pattern of the starting lithium amide. This minor contamination was reported also in the previous studies,^{19,20} on the other hand, no traces of LiOH or of other impurities were observed.

Being a powdered sample, DINS measures the spherically averaged PMD. The detailed experimental procedures to extract the PMD from DINS data can be found in Refs. 21–24, where data reduction and line shape analysis procedures are described in details.

III. COMPUTATIONAL DETAILS

Simulations were performed using a supercell containing 192 atoms (Fig. 1), which were arranged according to the

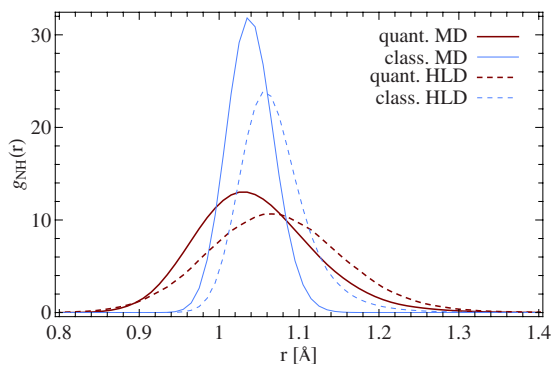


FIG. 2. (Color online) Comparison between the intramolecular peak of the N-H radial distribution function, as computed from MD and harmonic lattice dynamics (HLD) (Ref. 30) with and without considering nuclear quantum effects. Note that because of strong anharmonicities the classical HLD provides an unsatisfactory description of this system. A similar discrepancy is found when comparing the quantum thermostat results and HLD with Bose-Einstein occupations.

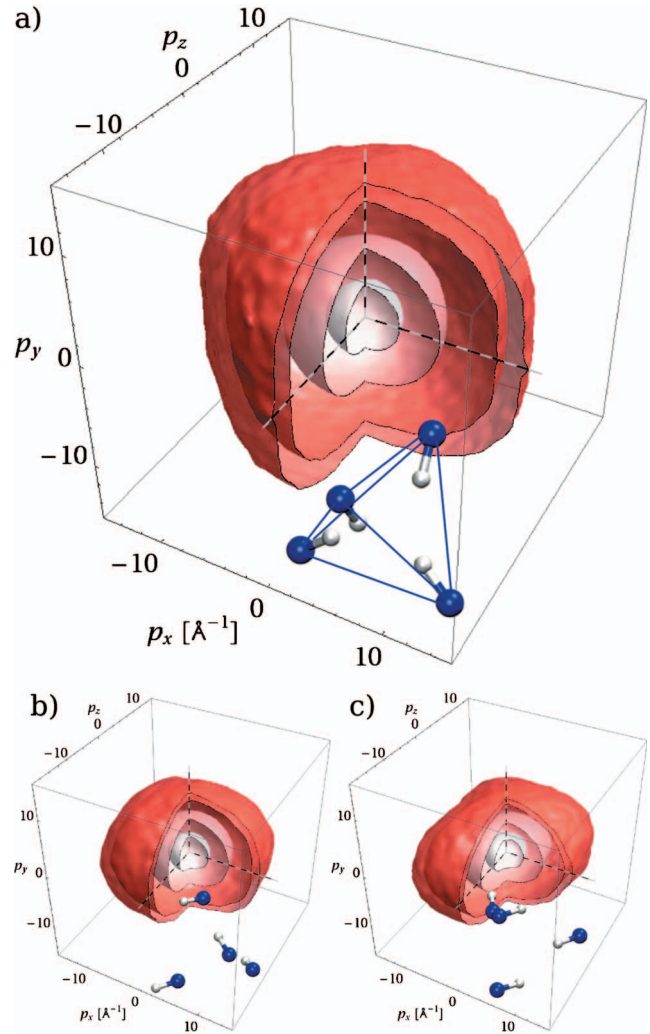


FIG. 3. (Color) (a) Three-dimensional proton momentum distribution for the low-temperature phase of lithium imide described in Ref. 25. Isosurfaces enclose 95%, 90%, 50%, and 10% of the probability density. The arrangement of the hydrogen atoms around a Li vacancy, aligned along the $\langle 111 \rangle$ axes, is also reported, relative to the Cartesian reference. (b) The three-dimensional PMD for the structure of Ref. 31 and (c) for the one reported in Ref. 32 are also reported for comparison, together with exemplary representation of the orientation of NH bonds. The $Pbca$ and $Pnma$ phases were modeled by a supercell with 64 atoms, at the theoretical equilibrium lattice parameters reported in Refs. 31 and 32.

partially disordered structure which was recently proposed as a model of the low-temperature, $Fd\bar{3}m$ phase of Li_2NH .²⁵ In this structure, Li atoms occupy the tetrahedral sites of the fcc lattice of nitrogen atoms. Two types of Li vacancies with different local symmetry are present. One kind of vacancy is tetrahedrally coordinated by N-H groups while the second one is tetrahedrally coordinated by Li interstitials. These tetrahedral clusters of Li interstitials are found to stabilize the structure considerably, and are distributed in a disordered way, resulting in an excellent match with experimental diffraction data.^{25,26} Moreover, they hinder the mobility of Li interstitials, which would be very high if the clusters were broken.²⁵ Starting from this structure we performed Born-

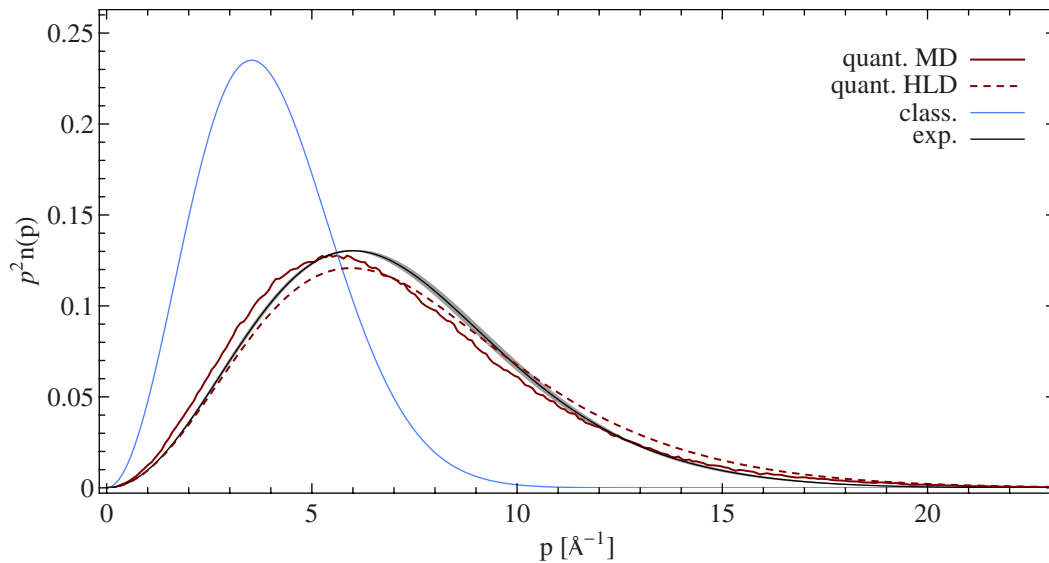


FIG. 4. (Color online) Comparison between the spherically averaged proton-momentum distribution expected for a classical system and from harmonic lattice dynamics at $T=300$ K (see Appendix), the PMD measured from a lithium imide sample and that computed from quantum-thermostatted molecular dynamics. The (small) error bars of experimental data are reported as a shading around the experimental curve.

Oppenheimer molecular-dynamics simulations within density-functional theory with gradient corrected exchange and correlation functional²⁷ as implemented in the CPMD (Ref. 28) package. Technical details of the calculations are the same as those used in Ref. 25. Thermal averages were performed over 15 ps of trajectory, following 5 ps used for equilibration at $T=300$ K.

Nuclear quantum effects were treated by means of a quantum thermostat, which is based on a bespoke generalized Langevin equation containing correlated noise. This stochastic process is designed to mimic the quantum-mechanical phase space distribution in the harmonic limit. The resulting nonequilibrium dynamics samples a stationary distribution which is a good approximation of the quantum mechanical one also in fairly anharmonic systems. This result is achieved without requiring any preliminary information, except for an upper-bound estimate of the stiffest vibrational mode present. We used the set of parameters qt-50_6, which can be downloaded from an on-line repository.²⁹ We refer the reader to Refs. 7 and 29 for further details.

IV. THEORETICAL AND EXPERIMENTAL RESULTS

Before discussing the comparison with the experimental proton momentum distribution, it is necessary to stress that the presence of anharmonic wagging modes of the imide groups makes a quasiharmonic treatment inappropriate. This is apparent in Fig. 2, where we compare the radial distribution function of the N-H group as computed from molecular dynamics and from the harmonic normal modes. The same figure also highlights the importance of nuclear quantum effects, which modify dramatically the typical fluctuations of the imide bonds.

While hydrogen and the stretching mode, in particular, exhibit the largest deviations from classical behavior, lithium

and nitrogen are also light nuclei and are therefore subject to nuclear quantum effects, albeit to a lesser extent. For instance, the average kinetic temperature computed during the quantum-thermostatted dynamics deviates from the classical value, and is 415 K for Li atoms, 410 K for N (which is heavier but participates into the stiff N-H stretching mode) and 858 K for the protons. These deviations illustrate the importance that nuclear quantum effects have in determining the properties of Li_2NH , such as the temperature at which the transition between the low-temperature and high-temperature phases occurs.²⁶

Computing the proton momentum distribution from the quantum-thermostatted dynamics is straightforward. In fact, the thermostat has been designed to yield the correct momentum and position distribution in the harmonic limit, and has proven to work also in the anharmonic case. Thus we only need to collect the momentum histogram to obtain the three-dimensional PMD, which is plotted in Fig. 3. The anisotropy of $n(\mathbf{p})$, which is a purely quantum mechanical effect, reflects the symmetry of the local environment of protons inside the crystal, with the bonds aligned along $\langle 111 \rangle$ directions of the nitrogen antiferroite sublattice, pointing toward Li vacancies.^{25,26,33} While we could not measure the directionally resolved $n(\mathbf{p})$ because of the difficulties in obtaining a single-crystal sample of appropriate dimensions, this result demonstrates the ease by which this quantity can be accessed by our computational technique, providing detailed information which can help to interpret experiments for other systems.³⁴

To compare with the powder sample experimental data, we spherically averaged the three dimensional PMD. As it can be seen from Fig. 4, there is a satisfactory agreement between experiments and theory. In particular, we observe that quantum-thermostatted simulations match experimental data better than the results from the quantum harmonic approximation, even if the effects of anharmonicity are less

pronounced than in the case of the N-H radial distribution function (see Fig. 2). To quantify the discrepancy with experiments, and to extract information relevant to the structural model of Li_2NH , we fitted the experimental and theoretical PMD's with a anisotropic Gaussian model. We assumed a different spread in the directions parallel and perpendicular to the N-H bond,^{35,36} resulting into

$$n(\mathbf{p}) \propto \exp\left(-\frac{p_z^2}{2\sigma_{\parallel}^2} - \frac{p_x^2 + p_y^2}{2\sigma_{\perp}^2}\right), \quad (1)$$

which was then spherically averaged.

The resulting fit matches both curves very well, with values of adjusted R^2 greater than 0.999. The fit yields the parameters $\sigma_{\parallel}=6.49 \text{ \AA}^{-1}$ and $\sigma_{\perp}=3.15 \text{ \AA}^{-1}$ for the theoretical PMD, and $\sigma_{\parallel}=5.77 \text{ \AA}^{-1}$ and $\sigma_{\perp}=3.70 \text{ \AA}^{-1}$ for the experimental one.

The discrepancy is certainly larger than the experimental error bar, however the anisotropy in the PMD is correctly captured, and the spread in the direction parallel and perpendicular to the bond is qualitatively reproduced. This is indeed a remarkable result for an approximate model of nuclear quantum effect such as the one used in the present work, which can be applied with no computational overhead with respect to standard *ab initio* molecular dynamics. While it is difficult to assess the uncertainty in our theoretical results, a possible approach to gauge the error is to repeat simulations with a different set of noise parameters. We did so using the parameters qt-20_6,²⁹ and obtained $\sigma_{\parallel}=6.31 \text{ \AA}^{-1}$ and $\sigma_{\perp}=3.40 \text{ \AA}^{-1}$. The comparison with the results obtained using qt-20_6 sets a lower bound for the error at about 10%. The difference in the local symmetry for different structures proposed for Li_2NH (Refs. 25, 26, 31, and 32) reflects in sizable differences between the corresponding three-dimensional $n(\mathbf{p})$ (cf. Fig. 3). Unfortunately these differences are smeared out by the spherical averaging, making our error bars too large to discriminate between the different candidates based solely on the spherically averaged distribution. However, for the reasons discussed in our previous work,²⁵ the other proposed structures have to be dismissed because of worse agreement with diffraction data.

V. CONCLUSIONS

In this paper we have shown how a recently developed method to compute nuclear quantum effects can be used together with *ab initio* molecular dynamics to model complex materials containing light atoms. Our method involves negligible overhead with respect to conventional *ab initio* MD, whereas a treatment of nuclear quantum effects by path integral methods would have implied at least a tenfold increase in computational effort. We were therefore able to use a large simulation cell, which was mandatory for Li_2NH to reproduce the experimental structure of the low-temperature phase. We obtained good agreement with the experimental proton momentum distribution, a result of great significance given the growing importance of inelastic neutron-scattering

experiments as a sensitive probe of the local environment in hydrogen-containing materials. Both experimental and theoretical data are perfectly fitted by a model in which imide groups perform hindered librations.

The possibility of treating delicate nuclear quantum effects inexpensively, albeit approximately, suggests that the quantum thermostat should be used whenever light atoms are present, and a more accurate treatment by path-integral methods is unfeasible because of the excessive computational effort. Together with accurate first-principles calculations of the interatomic forces, this will shed light on the role of nuclear quantum effects in condensed-phase systems.

Note added in proof: It has been brought to our attention that an ordered structure similar to the one we proposed in Ref. 25 and we use in this work has been obtained by another group³⁷ by an extensive search of candidate crystal structures. This substantiates further our choice of the structural model for Li_2NH .

ACKNOWLEDGMENTS

R. Senesi and J. Mayers are gratefully acknowledged for suggestions during data reduction and analysis. We thank C. Andreani for useful discussions. One of the authors (A.P.) acknowledges the CNISM-CNR research program.

APPENDIX: COMPUTATION OF THE PROTON MOMENTUM DISTRIBUTION WITHIN HARMONIC LATTICE DYNAMICS

The computation of the quantum-mechanical proton momentum distribution within harmonic lattice dynamics is straightforward, but we report here the procedure, for completeness. At first, we observe that the quantum momentum distribution can be written as a multivariate Gaussian, with frequency-dependent widths along the same normal modes which can be obtained by classical lattice dynamics. Let the indexes i , k , and α label atoms, phonons, and Cartesian coordinates, respectively, and ω_k and $e_{i\alpha}^{(k)}$ be the frequency and the components of the k th normalized eigenvector of the dynamical matrix. The covariance matrix which describes the multivariate-Gaussian distribution of momenta at temperature T reads

$$\langle p_{i\alpha} p_{j\beta} \rangle = \hbar \sqrt{m_i m_j} \sum_k e_{i\alpha}^{(k)*} e_{j\beta}^{(k)} \frac{\omega_k}{2} \coth \frac{\hbar \omega_k}{2k_B T}.$$

Then, one must consider that the scattering is incoherent, and will result from the superposition of the contributions of individual protons, which are described by the marginal probability distribution, which is given by the 3×3 matrices $C_{\alpha\beta}^{(i)} = \langle p_{i\alpha} p_{i\beta} \rangle$. The three-dimensional PMD finally reads

$$n(\mathbf{p}) \propto \sum_i \frac{1}{\sqrt{\det(\mathbf{C}^{(i)})}} e^{-(1/2)\mathbf{p}^T [\mathbf{C}^{(i)}]^{-1} \mathbf{p}},$$

which can be spherically averaged to give $n(p)$.

*michele.cerriotti@phys.chem.ethz.ch

- ¹R. P. Feynman and A. R. Hibbs, *Quantum Mechanics and Path Integrals* (McGraw-Hill, New York, 1964).
- ²D. M. Ceperley, *Rev. Mod. Phys.* **67**, 279 (1995).
- ³D. Marx and M. Parrinello, *J. Chem. Phys.* **104**, 4077 (1996).
- ⁴D. Marx, M. E. Tuckerman, J. Hutter, and M. Parrinello, *Nature (London)* **397**, 601 (1999).
- ⁵M. Ceriotti, G. Bussi, and M. Parrinello, *Phys. Rev. Lett.* **102**, 020601 (2009).
- ⁶M. Ceriotti, G. Bussi, and M. Parrinello, *Phys. Rev. Lett.* **103**, 030603 (2009).
- ⁷M. Ceriotti, G. Bussi, and M. Parrinello, *J. Chem. Theory Comput.* **6**, 1170 (2010).
- ⁸J. A. Morrone and R. Car, *Phys. Rev. Lett.* **101**, 017801 (2008).
- ⁹L. Lin, J. A. Morrone, R. Car, and M. Parrinello, *Phys. Rev. Lett.* **105**, 110602 (2010).
- ¹⁰C. Andreani, D. Colognesi, J. Mayers, G. F. Reiter, and R. Senesi, *Adv. Phys.* **54**, 377 (2005).
- ¹¹P. Chen, Z. Xiong, J. Luo, J. Lin, and K. L. Tan, *Nature (London)* **420**, 302 (2002).
- ¹²P. Chen and M. Zhu, *Mater. Today* **11**, 36 (2008).
- ¹³<http://www.isis.rl.ac.uk>
- ¹⁴A. Pietropaolo, C. Andreani, A. Filabozzi, E. Pace, and R. Senesi, *Nucl. Instrum. Methods* **570**, 498 (2007).
- ¹⁵E. Schooneveld, J. Mayers, N. Rhodes, A. Pietropaolo, C. Andreani, R. Senesi, G. Gorini, E. Perelli-Cippo, and M. Tardocchi, *Rev. Sci. Instrum.* **77**, 095103 (2006).
- ¹⁶G. Reiter and R. Silver, *Phys. Rev. Lett.* **54**, 1047 (1985).
- ¹⁷V. F. Sears, *Phys. Rev. B* **30**, 44 (1984).
- ¹⁸R. Senesi, D. Colognesi, A. Pietropaolo, and T. Abdul-Redah, *Phys. Rev. B* **72**, 054119 (2005).
- ¹⁹Y. Kojima and Y. Kawai, *J. Alloys Compd.* **395**, 236 (2005).
- ²⁰T. Noritake, H. Nozaki, M. Aoki, S. Towata, G. Kitahara, Y. Nakamori, and S. Orimo, *J. Alloys Compd.* **393**, 264 (2005).
- ²¹A. Pietropaolo, C. Andreani, A. Filabozzi, R. Senesi, G. Gorini, E. Perelli-Cippo, M. Tardocchi, N. Rhodes, and E. Schooneveld, *J. Instrumentation* **1**, P04001 (2006).
- ²²A. Pietropaolo, D. Fernandez-Canoto, E. Perelli-Cippo, S. Diré, and P. Proposito, *Phys. Rev. B* **77**, 014202 (2008).
- ²³A. Pietropaolo, R. Senesi, C. Andreani, A. Botti, M. A. Ricci, and F. Bruni, *Phys. Rev. Lett.* **100**, 127802 (2008).
- ²⁴C. Pantalei, A. Pietropaolo, R. Senesi, C. Andreani, S. Imberti, J. Mayers, C. Burnham, and G. Reiter, *Phys. Rev. Lett.* **100**, 177801 (2008).
- ²⁵G. Miceli, M. Ceriotti, M. Bernasconi, and M. Parrinello, <http://arxiv.org/abs/1009.1488>
- ²⁶M. P. Balogh, C. Y. Jones, J. F. Herbst, L. G. Hector, Jr., and M. Kundrat, *J. Alloys Compd.* **420**, 326 (2006).
- ²⁷J. P. Perdew, K. Burke, and M. Ernzerhof, *Phys. Rev. Lett.* **77**, 3865 (1996).
- ²⁸<http://www.cpmc.org/>, Copyright IBM Corp 1990–2006, Copyright MPI für Festkörperforschung Stuttgart 1997–2001.
- ²⁹<http://gle4md.berlios.de>
- ³⁰J. Kohanoff, W. Andreoni, and M. Parrinello, *Phys. Rev. B* **46**, 4371 (1992).
- ³¹T. Mueller and G. Ceder, *Phys. Rev. B* **74**, 134104 (2006).
- ³²B. Magyari-Köpe, V. Ozoliņš, and C. Wolverton, *Phys. Rev. B* **73**, 220101(R) (2006).
- ³³L. G. Hector, Jr. and J. F. Herbst, *J. Phys.: Condens. Matter* **20**, 064229 (2008).
- ³⁴G. F. Reiter, J. Mayers, and P. Platzman, *Phys. Rev. Lett.* **89**, 135505 (2002).
- ³⁵G. Reiter, J. C. Li, J. Mayers, T. Abdul-Redah, and P. Platzman, *Braz. J. Phys.* **34**, 142 (2004).
- ³⁶V. Garbuio, C. Andreani, S. Imberti, A. Pietropaolo, G. Reiter, R. Senesi, and M. Ricci, *J. Chem. Phys.* **127**, 154501 (2007).
- ³⁷T. Mueller and G. Ceder, *Phys. Rev. B* **82**, 174307 (2010).